Electrical Engineering Technical Journal, ISSN: 3007-9772, Vol. 2, No. 1, 2025, Pages 1-10
DOI: https://10.51173/eetj.v2i1.12

Electrical Engineering Technical Journal
Journal homepage: http://eetj.mtu.edu.iq

RESEARCH ARTICLE

Power Allocation in Cell Free Massive MIMO System under Pilot Contamination

Mohammed Dawood Alrubay [1*], and Hayder Almosa [2]

[1] Department of Electrical Engineering, Faculty of Engineering, University of Kufa, Najaf, Iraq
[2] Department of Electronic and Communication Engineering, Faculty of Engineering, University of Kufa, Najaf, Iraq

[*] Corresponding Author Email: mohammedd.alrubay@student.uokufa.edu.iq

Article Info.

Article history:

Received
12 July 2024

Accepted
24 August 2024

Published in Journal
31 January 2025

Abstract

Cell-free massive MIMO technology holds significant promise as a pivotal enhancement for next-generation 5G and 6G networks. This technology features a network architecture where a single central processing unit oversees multiple access points, thereby enhancing wireless communication capacity and efficacy. By enabling broader connectivity beyond the confines of standard cellular networks, it minimizes signal interruptions and improves spectral efficiency. Despite these advancements, further research is necessary to define a comprehensive implementation strategy for deploying cell-free massive MIMO systems under real-world conditions. The Signal-to-Interference-plus-Noise Ratio (SINR) plays a crucial role in wireless communications. In this paper, the problem of power allocation is addressed under the assumption of pilot contamination. Pilot contamination occurs when multiple users share the same pilot signal. Specifically, two users were assumed to have the same pilot signal, which significantly decreased the SINR and increased the interference among these users. This reduction in SINR leads to potential degradation in achievable data rates and overall system performance. The proposed algorithm aims to reduce pilot contamination by solving a max-min optimization problem that insures fairness among all users. The proposed algorithm obtained the optimal power coefficient associated with each user by taking advantage of uplink-downlink duality and considering all interference terms in the calculations. The proposed algorithm finds out the optimal solution in an iterative manner until the feasible solution is achieved. The methodology introduced calculation of achievable rates based on SINR, which is essential for evaluating power allocation in cell-free massive MIMO systems. Specifically, we focus on downlink sum-rate maximization and compare the effectiveness of Zero-Forcing (ZF) precoder against Conjugate Beamforming (CB) precoder.

Keywords: Cell-free Massive MIMO; Power Optimization; Downlink Sum-rate Maximization; ZF Precoding; CB Precoding.

1. Introduction

Introduced in the literature as reference [1], cell-free massive MIMO is a distributed system devoid of cell boundaries, integrating all antennas into a singular cell entity. This novel concept faces practical hurdles, notably the connection of antennas to the central controller constrained by the capacity of the links. Cell-free massive MIMO systems, characterized by numerous single-antenna Access Points (APs) operating simultaneously to serve a smaller cohort of users on shared frequency resources. As shown in Figure 1, it has garnered significant interest due to their proficiency in delivering consistent, superior service quality to every user, thereby eliminating the need for handovers [2] [3] [4] [5]. Channel hardening refers to the phenomenon where the effect of small-scale fading diminishes as the number of antennas increases, leading to more predictable and stable channel conditions. Access points in cell-free massive MIMO systems provide the advantage of channel hardening, similar to conventional massive MIMO configurations, ensuring consistent service quality [6] [7] [8]. Exploiting the spatial domain for spectral efficiency gains is also employed in a technique known as beamforming [9]. In multi-antenna systems, accurate Channel State Information (CSI) is essential for successful transmission. Ideally, mutually orthogonal training sequences or pilots should be selected for precise channel estimation. However, in most real-world scenarios, there are more users than available orthogonal training sequences. Consequently, a single training sequence may be assigned to multiple users, resulting in pilot contamination, which significantly affects massive MIMO systems due to the reuse of non-orthogonal pilot sequences across neighboring cells. As the number of interfering cells increases, the severity of the problem escalates rapidly, potentially leading to system failures [10] [11]. Extensive research on pilot contamination exists within centralized massive MIMO systems [12] [14]. Certain characteristics of massive MIMO channels, such as advantageous propagation, channel hardening, or constrained angular spread, have been identified to mitigate pilot contamination. These techniques operate in the power domain [15], angular domain [16] [17], or a combination of both [18], effectively reducing or eliminating the issue. However, these beneficial channel traits are not preserved in distributed settings, making pilot contamination a persistent and complex challenge in cell-free massive MIMO systems. In this work, the problem of power allocation under pilot contamination in the downlink was investigated, and the CSI was calculated in the AP under pilot contamination using our previous work [19]. This approach facilitates coverage for numerous users over the same frequency resources. Massive MIMO systems are characterized by using a vast number of antennas to simultaneously accommodate a substantial number of users within the same frequency spectrum [20] [21]. Numerous studies have demonstrated that massive MIMO can substantially improve system performance by enhancing

spectral efficiency, increasing data rates, and providing better coverage [22] [23], making it a strong candidate for 5G technology [24] [25]. Research advancements have shown that antenna distribution throughout the cell, as opposed to central co-location, enhances key performance indicators such as spectral efficiency, transmission power requirements, and coverage area [26] [27]. Despite these benefits, these systems also face challenges [28]. Studies [20] [2] have explored the performance of CB and ZF precoders in cell-free networks, employing max-min power allocation to enhance system performance under varying network conditions. Pilot contamination, where non-orthogonal pilot signals from different users interfere during channel estimation, degrades system performance. The max-min power allocation strategy in CB is utilized to bolster system performance, encompassing a non-convex optimization problem with significant computational demands. For the ZF precoder considering channel estimation errors, we advocate for less complex power allocation algorithms (expounded in Section 5). This work contributes to operationalizing cell-free massive MIMO by proposing a local coverage model and optimizing the sum rate. This paper delineates a technique based on the SINR to address the downlink sum-rate maximization problem, providing a detailed algorithm and performance analysis. CB precoding aligns the transmitted signal with the intended user's channel vector, maximizing received signal power but may result in higher interference in densely populated networks. The ZF algorithm significantly outperforms CB in terms of achievable sum-rate and interference mitigation.

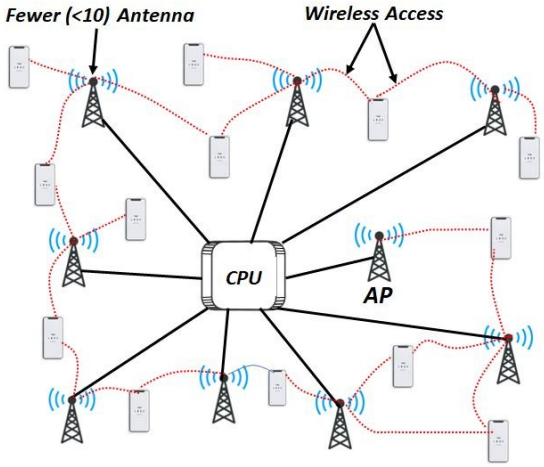

Fig. 1. Cell-free massive MIMO.

The structure of this paper is methodically arranged as follows. System Model (Section 2): An examination of the essential elements of our cell-free massive MIMO system is conducted. Channel Estimation (Section 3): This section is dedicated to a detailed analysis of channel estimation methodologies. Downlink Achievable Rate and Optimal Power Allocation (Sections 4, 5): An in-depth exploration of the proposed optimization algorithm is presented. Numerical results and discussions (Section 6): Empirical data are showcased, followed by a series of analytical discussions. Conclusion (Section 7). The paper culminates with a synthesis of our investigative efforts and an outline of prospective avenues for further research.

2. System Model

In this work, a cell-free network model is developed and analyzed, which eliminates internal cell divisions and consolidates the network into a single large cell with P access points and U users, each equipped with an individual antenna. This model builds upon the foundational work of [29]. All access points, also termed antennas in this discourse, serve the entire user base and are linked to a network control unit. The channel coefficient for an antenna p and user u is specified as follows [1]:

$$q_{pu} = \sqrt{\beta_{pu}} g_{pu} \tag{1}$$

In the context of signal propagation, the term β_{pu} denotes the coefficient associated with large-scale fading. This coefficient is pivotal in quantifying the diminution of signal power, commonly referred to as path loss, and encompasses the shadowing effects. The latter is distinguished by a coefficient that demonstrates a slow fluctuation over time. It is feasible to monitor and forecast this coefficient with a reasonable level of precision. Contrary to systems that are co-located, a cell-free system is subject to large-scale fading. Notably, the extent of large-scale fading is unique for each combination of user and access point. The second component, denoted as g_{pu}, follows a complex normal distribution, $g_{pu} \sim \mathcal{CN}(0,1)$, and represents the coefficient of small-scale fading. These coefficients are regarded as random variables that are identically distributed and independent of each other. In accordance with the block fading model, it is postulated that g_{pu} $(1 \leq p \leq P, 1 \leq u \leq U)$ remains constant within a coherent interval and changes independently across different coherent intervals. Furthermore, the channel coefficients for uplink and downlink broadcasts are thought to be the same, a concept known as channel reciprocity. The channel matrix, which establishes the connection between each antenna and user, is represented by $Q \in C^{P \times U}$, where the element $[Q]_{pu} = q_{pu}$.

3. Channel Estimation

In a massive MIMO system devoid of cellular divisions, it is assumed that $P \geq U$. CSI refers to the known channel properties, such as channel coefficients, which describe how signals propagate from the transmitter to the receiver. Accurate CSI is essential for optimizing signal transmission and achieving high throughput in wireless communication systems. Consequently, antenna p is tasked with the computation of the channel coefficients g_{pu} , $u = 1, \cdots, U$. Accurate channel estimation is facilitated through the employment of the Time Division Duplex (TDD) protocol, which has been shown in previous studies [1] to be effective in environments similar to our proposed model. Within this framework, each user transmits an initial training signal $\varphi_1, \cdots, \varphi_U$ to the antennas in unison. Subsequently, the protocol entails the derivation of channel coefficients for each antenna and the utilization of these determinations to direct beamformed

data to every user. Approximately 1400 pilots, exhibiting mutual orthogonality and utilizing half of the coherence time, are operational provided the users' velocity does not exceed 10 km/h and the carrier frequency stands at 1.9 GHz. It is thus rational to infer that users who recycle the same training signal are spatially separated, mitigating the risk of significant pilot contamination namely, the coherent interference resulting from multiple users employing identical pilot sequences. Hence, it is postulated that pilot sequences of sufficient length to ensure mutual orthogonality, $\tau \geq U$, i.e. $\varphi_i^H \varphi_j = \delta_{ij}$, are allocated to users, non-orthogonal training signals of length $\tau \geq U$,where $\varphi_i^H \varphi_j = \delta_{i\neq j}$. This approach incorporates a direct consideration of the noise-induced error in channel estimation. During the training phase at antenna p, the sequence of signals received is given as [1][2].

$$y_p = \sqrt{\rho_r \tau} \sum_{i=1}^{U} q_{pi} \varphi_i + n_p \tag{2}$$

In this scenario, ρ_r represents the power of the uplink signal, while n_p, which is distributed as $n_p \sim \mathcal{CN}(0, I_\tau)$, signifies the Additive White Gaussian Noise (AWGN). The Minimum Mean Square Error (MMSE) estimation of q_{pu} is determined accordingly as [1]:

$$\hat{q}_{pu} = \frac{\sqrt{\rho_r \tau}\ \beta_{pu}}{1+\rho_r \tau \beta_{pu}} \varphi_u^H y_p \tag{3}$$

Let $\tilde{q}_{pu} = q_{pu} - \hat{q}_{pu}$ be the channel estimate error. It is well known that there isn't any relationship between $\hat{q}_{nu}$ and $\tilde{q}_{pu}$, As explained in[1][2][29]

$$\hat{q}_{pu} \sim C\mathcal{N}\left(0, \frac{\rho_r \tau\ \beta_{pu}^2}{1+\rho_r \tau\ \beta_{pu}}\right) \tag{4}$$

$$\tilde{q}_{pu} \sim C\mathcal{N}\left(0, \beta_{pu} - \frac{\rho_r \tau\ \beta_{pu}^2}{1+\rho_r \tau\ \beta_{pu}}\right) \tag{5}$$

The channel coefficients were obtained in this work using our method in previous work which deals with pilot contamination when two users share the same pilot signal [19]. In the subsequent sections, we will conduct an analysis of the primary linear precoding strategies, focusing specifically on zero-forcing precoding. As previously noted in Section I, our discussion throughout this paper is centered on addressing the max-min optimization problems.

4. Downlink Achievable Rate

ZF precoding is a linear precoding technique where the transmitted signal is designed to cancel interference with other users by inverting the channel matrix. This ensures that each user's signal is received with minimal interference from other users, improving overall system performance. In the absence of a specified power allocation, the ZF precoder is characterized by a unique matrix. Concurrently, the objective of this discourse is to ascertain the optimal power allocation method for the ZF precoder within a cell-free massive MIMO framework. It is presupposed that every user falls within the coverage area of each antenna, and the signal emanating from all access points is distinctly defined.

$$x_p = Z_f R v \tag{6}$$

Where Z_f represents the precoding matrix, R denotes the diagonal power matrix, which contains the square roots of power allocations, $\sqrt{\eta_1}, \sqrt{\eta_2}, \ldots, \sqrt{\eta_t}$, along its diagonal, and v is the vector that comprises the transmitted symbols for all users. In the assumption of employing a ZF precoder, it is established that [30]:

$$Z_f = \widehat{Q}^*(\widehat{Q}^T \widehat{Q}^*)^{-1} \tag{7}$$

Within this framework, the symbol $\widehat{Q}^*$ denotes an estimated version of the channel matrix Q. By applying the matrix Z_f, we accomplish $\widehat{Q}^T Z_f = I_U$, where I_U is the identity matrix. The variablesα_{pu}, $1 \leq p \leq P, 1 \leq u \leq U$, are the individual elements of Z_f. The matrix Z_{ZF} is defined as the precoding matrix tailored for the challenge of cell-free power allocation, where each element $[Z_{ZF}]_{pu} = \alpha_{pu}^{ZF}$, and defined as follow [30].

$$\alpha_{pu}^{ZF} = \sqrt{\rho_d \eta_{pu}}\, \alpha_{pu} \quad p = 1, \cdots, P, u = , \cdots, U \tag{8}$$

To guarantee that the matrix product $\widehat{Q}^T Z_{ZF}$ is diagonal, it is crucial to ensure that the power coefficients $\eta_{1u}, \ldots, \eta_{Pu}$, foru $= 1 \cdots, U$, are properly aligned. Therefore, we proceed with the hypothesis that these power coefficients are uniquely determined by the variable t, implying that $\eta_{pt} = \eta_t$. Based on this assumption, we then define the precoding matrix in a manner that is consistent with these conditions.

$$Z_{ZF} = \widehat{Q}^*(\widehat{Q}^T \widehat{Q}^*)^{-1} R \tag{9}$$

By using the zero-forcing property (9), the equation becomes:

$$\hat{q}_u^T Z_f R v = \sqrt{\rho_d \eta_u}\, v_u \tag{10}$$

Within the context of channel estimation errors, noise and interference are taken into account as shown in the following equation. The following term describes the interference effects brought on by inaccurate channel estimation:

$$\tilde{q}_u^T Z_f R v \tag{11}$$

With the zero-forcing condition (9) in mind, the interference phrase may be expressed as follows:

$$\sqrt{\rho_d}\, \tilde{q}_u^T \widehat{Q}^*(\widehat{Q}^T \widehat{Q}^*)^{-1} R v \tag{12}$$

The received signal at the u^{th} user is given by

$$y_u = q_u^T x_p + n_u$$
$$= (\hat{q}_u + \tilde{q}_u)^T Z_f Rv + n_u \quad (13)$$

We may define the connection as follows in the case where n_u indicates the Gaussian noise with distribution $n_u \sim \mathcal{CN}(0, \sigma^2)$. The precoder's zero forcing attribute allows for additional simplification of the aforementioned relation.

$$y_u = \hat{q}_u Z_f Rv + \tilde{q}_u Z_f Rv + n_u$$
$$= \underbrace{\sqrt{\rho_d \eta_u}\, v_u}_{\text{Part1}} + \underbrace{\sqrt{\rho_d}\, \tilde{q}_u^T \hat{Q}^* (\hat{Q}^T \hat{Q}^*)^{-1} Rv}_{\text{Part2}} + \underbrace{n_u}_{\text{Part3}} \quad (14)$$

The term part 1 denotes the intended signal for the user indexed by u^{th}. Part 2 is used to describe the interference that stems from the estimated channel error, while part3 signifies the noise at the receiver. For massive MIMO systems, a general capacity lower bound has been determined in [31], while for cell-free systems, a more detailed bound is provided in [2]. Using our notation. Consequently, the SINR for the user at position u^{th} can be calculated as follows:

$$SINR_u = \frac{\mathbb{E}\left[\left|\sqrt{\rho_d \eta_u}\, v_u\right|^2\right]}{\mathbb{E}\left[\left|\sqrt{\rho_d}\, \tilde{q}_u^T \hat{Q}^* (\hat{Q}^T \hat{Q}^*)^{-1} Rv\right|^2\right] + \sigma^2} \quad (15)$$

Utilizing the characteristics of expected values and acknowledging that $\tilde{q}_u$ adheres to The Gaussian distribution is complicated with the parameters $\tilde{q}_u \sim \mathcal{CN}(0, \beta_{pu} - \alpha_{pu})$, the formula for the SINR can be distilled into a more straightforward expression as follows:

$$SINR_u = \frac{\rho_d \eta_u}{\rho_d \sum_{i=1}^{P} \eta_t B_{ui} + \sigma^2} \quad (16)$$

The interference factors resulting from inaccuracies in channel estimate are captured in matrix B to be more precise, the expression for every element $[B]_{ui}$ is as follows:

$$B_{ui} = \sum_{p=1}^{P} (\beta_{pu} - \alpha_{pu}) \left[\left(\hat{Q}^T \hat{Q}\right)^{-1}\right]_{ui} \quad (17)$$

As a result, we possess:

$$SINR_u = \frac{\rho_d \eta_u}{\rho_d (B\eta)_u + \sigma^2} \quad (18)$$

Where, β_{pu} is the large-scale fading coefficient between the u^{th} user and P^{th}access point. The error in the channel estimation is explained by $\alpha_{pu} = \frac{\rho_r \tau \beta_{pu}^2}{1 + \rho_r \tau \beta_{pu}}$, the channel matrix estimation is denoted by $\hat{Q}$. The Gram matrix of the estimated channel matrix is $\hat{Q}^T \hat{Q}$. The reverse representation of the Gram matrix is $\left(\hat{Q}^T \hat{Q}\right)^{-1}$. The diagonal elements of the product matrix $\left(\hat{Q}^T \hat{Q}\right)^{-1}$ represent the orthogonality properties used in zero-forcing.

5. Optimal Power Allocation

To maximize the cumulative rate of users, which is a crucial system performance metric, we need to solve the following optimization problem:

$$\max_{\eta} \sum_{u=1}^{U} \log_2 \left(1 + \frac{\rho_d \eta_u}{\rho_d (B\eta)_u + \sigma^2}\right) \quad (19)$$

The constraint $\sum_U \eta_u \leq R_{total}$, $\eta \geq 0$

The issue is rewritten to maximize the lower SINR across all users, instead of aiming for the direct maximizing of the total rate. This method encourages computational viability as well as fairness. The revised goal might be stated in the following manner:

$$SINR_u = \frac{\rho_d \eta_u}{\rho_d (B\eta)_u + \sigma^2} \quad (20)$$

Problem of max-min power allocation, given the power constraints per antenna, is given by

$$\max_{\eta} \min_{u} \frac{\rho_d \eta_u}{\rho_d (B\eta)_u + \sigma^2} \quad (21)$$

As indicated in [30], the zero-forcing precoder's capability to nullify interference caused by transmissions to other users must be preserved. The power transmitted from antenna p to user u although the power coefficients are solely functions of u ,$\rho_d \left|\alpha_{pu}^{ZF}\right|^2 = \rho_d \eta_u \left|\alpha_{pu}\right|^2$ is contingent upon both p andu . The denominator and numerator of $SINR_u$ in equation (21) are linear functions of η . Given that $SINR_u$ is a

quasiconcave function, equation (21) can be resolved employing the bisection method once again. Utilizing the principle of uplink-downlink duality, we acquire crucial insights that facilitate a more effective resolution of the power distribution dilemma. The duality concept proposes that the optimal resolution for the downlink beamforming challenge can be ascertained by first tackling an analogous uplink problem. This corresponding uplink predicament involves the maximization of the minimal SINR in the uplink, which is articulated as follows:

$$\mathrm{SINR_u}^{\mathrm{uplink}} = \frac{\rho_{u\mathrm{u}}}{\sum_{\mathrm{j}\neq\mathrm{u}}^{\mathrm{U}} \rho_{u} + \sigma^2} \tag{22}$$

Where $\rho_{u\mathrm{u}}$ is the uplink power assigned to user u.The bisection approach [32] may be employed, given that the issue in (21) is quasi-concave [2]. To utilize the bisection approach, the comparable problem is first defined as follows:

$$\max_{\eta} \min_{\mathrm{u}} \frac{\eta_{\mathrm{u}}}{(\mathrm{B}\eta)_{\mathrm{u}} + \frac{\sigma^2}{\rho_{\mathrm{d}}}} \tag{23}$$

To make this simpler, we add an auxiliary variable t to represent the minimal SINR, where $\max_{\eta,\mathrm{t}} \mathrm{t}$ subject to

$$\frac{\eta_{\mathrm{u}}}{(\mathrm{B}\eta)_{\mathrm{u}} + \frac{\sigma^2}{\rho_{\mathrm{d}}}} \geq \mathrm{t}, \forall \mathrm{u} \tag{24}$$

$$\sum_{\mathrm{i}=1}^{\mathrm{U}} \eta_{\mathrm{u}} \leq \mathrm{R_{total}}\ , \eta_{\mathrm{u}} \geq \mathrm{t}, \forall \mathrm{u} \tag{25}$$

The bisection method, along with alternative convex optimization techniques such as pilot assignment , has been proven effective in addressing quasi-convex optimization problems in prior research [33]. This study leverages these methods to optimize power allocation in cell-free massive MIMO systems. Furthermore, Algorithm 1 provides a systematic approach to solving the optimization issue, ensuring convergence to the optimal power allocation strategy.

Algorithm 1 Bisection Algorithm for Optimal Power Allocation

1: Input:
2: U ← Number of users
3: ρ ← Power constraint
4: σ^2 ← Noise variance
5: β_{pu} ← Large-scale fading coefficients
6: $\alpha_{\mathrm{pu}} \leftarrow \frac{\rho_r\ \tau\ \beta_{\mathrm{pu}}^2}{1+\rho_r\ \tau\ \beta_{\mathrm{pu}}}$
7: $\mathrm{R_{total}}$ ← Total power budget
8: P ← Number of antennas
9: Compute the interference matrix B
10: $\mathrm{B} \leftarrow 0_{\mathrm{u}\times\mathrm{u}}$
11: for u = 1 to U do
12: for i = 1 to T do
13: for p = 1 to P do
14: $\mathrm{B(u,i)} \leftarrow \mathrm{B(u,i)} + (\beta_{\mathrm{pu}} - \alpha_{\mathrm{pu}})/(\hat{q}_{\mathrm{ui}}' * \hat{q}_{\mathrm{u}})$
15: end for
16: end for
17: end for
18: Bisection Method Initialization
19: l ← 0
20: n ← $1e^4$
21: ∈ ← $1e^{-3}$
22: while $(\mathrm{n} - \mathrm{l}) \geq \in$ do
23: $\mathrm{t} \leftarrow (\mathrm{l} + \mathrm{n})/2$
24: CVX Optimization
25: Solve the following problem:
26: maximize t
27: subject to:
28: $\frac{\eta_{\mathrm{u}}}{\mathrm{B(u,:)}\eta + \frac{\sigma^2}{\rho_{\mathrm{d}}}} \geq \mathrm{t}, \forall \mathrm{u}$
29: $\sum_{\mathrm{i}=1}^{\mathrm{U}} \eta_{\mathrm{u}} \leq \mathrm{R_{total}}$
30: $\eta_{\mathrm{u}} \geq \mathrm{t}, \forall \mathrm{u}$
31: if the problem is feasible then
32: $\mathrm{n} \leftarrow \mathrm{t}$
33: $\eta_{\mathrm{opt}} \leftarrow \eta$
34: else
35: $\mathrm{l} \leftarrow \mathrm{t}$
36: end if
37: end while
38: Output:
39: η_{opt} ← optimal power allocation

6. Numerical Results

In our research, we examine a densely populated area measuring 2 x 2 km², implementing wrap-around techniques to mitigate border effects. It is postulated that P access points and U users are distributed randomly throughout this region. We use the COST Hata model for the large-scale fading coefficients [1].

$$10\log_{10}\beta_{pu} = -136 - 35\log_{10}(d_{pu}) + s_{pu} \quad (26)$$

In the given context, d_{pu} represents the distance in kilometers between antenna p and user u, and $s_{pu} \sim \mathcal{N}(0, \sigma^2_{shad})$, where $\sigma_{shad} = 8$. The variance of the receiver noise is denoted as $\sigma^2_n = 290 \times \mathcal{K} \times \mathcal{B} \times \mathcal{NF}$, with $\mathcal{B}, \mathcal{K}$, and $\mathcal{NF}$ signifying the bandwidth (20MHz), Boltzmann's constant, and the noise figure (9 dB), respectively.

TABLE 1: Simulation parameters.

Parameters	Values
Standard deviation shadowing	8 dB
Power transmitted by every U	20 dBm
AP radiated power	30 dBm
frequency of carriers	1.9 GHz
The bandwidth	20 MHz
Noise figure	9 dB
Thermal noise level	- 174 dB m\Hz
Height of the AP antenna	15 m
Height of the U antenna	1.65 m
d_1	50 m
d_0	10 m
P	128
U	16

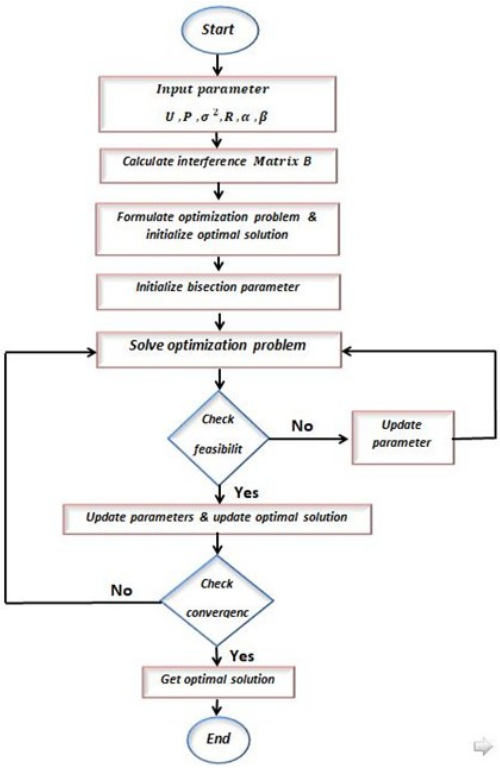

Fig. 2. Flowchart of the proposed power allocation algorithm.

This study presents the empirical cumulative distribution functions (CDFs) of per-user rates, comparing the use of uniform power coefficients and max-min power allocation in cell-free massive MIMO configurations. In this context, P is set to 128 and U is set to 16. Figure 2 represents the flowchart of the proposed algorithm for our system model.

Figure 3 depicts the relationship between the downlink achievable rate, measured in (bits/sec/Hz), and the quantity of APs within a cell-free network, comparing two distinct precoding strategies. The ZF precoding method demonstrates a marked superiority over the CB approach regarding the downlink achievable rate for all evaluated AP quantities. For instance, at a deployment of 200 APs, the ZF precoder initiates with an achievable rate of roughly 284 bits/sec/Hz, in contrast to the CB precoder, which commences at approximately 62.7 bits/sec/Hz. This disparity suggests that the ZF precoder is highly effective in reducing interference, thereby enhancing spectral efficiency, particularly as the network becomes more saturated with an increasing number of APs. Furthermore, the performance differential between the ZF and CB precoders expands in tandem with the AP count, underscoring the ZF precoder's enhanced capability to mitigate interference in densely populated network environments.

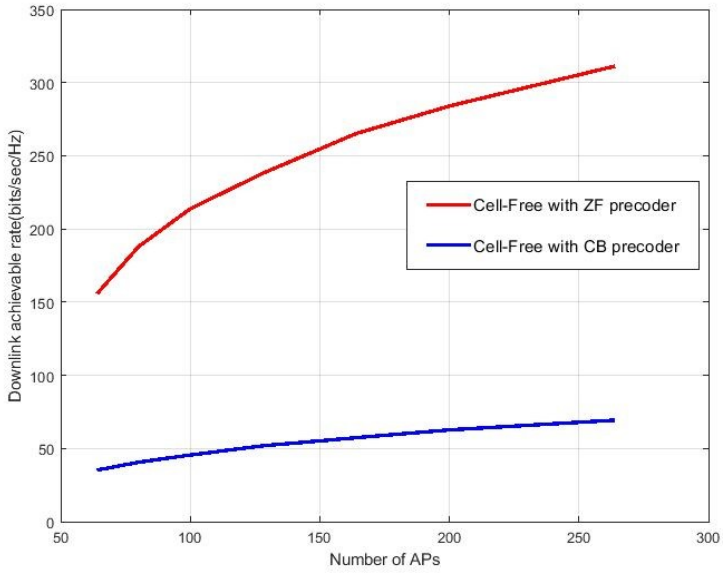

Fig. 3. Shows a downlink achievable rate between the proposed (ZF) precoding technique and the conventional (CB) precoding method against the number of Aps.

Figure 4 illustrates scenarios with a higher user count, while Figure 5 depicts scenarios with a lower user count. Both figures examine the CDF of the sum-rate for two precoding strategies within a cell-free massive MIMO system, assessing performance across varying user densities. It is observed that the ZF precoder consistently surpasses the CB precoder in environments with both high and low user densities. The sum-rate attained using the ZF precoder is notably superior, underscoring its efficiency in interference mitigation and optimal spectrum utilization. These findings highlight the criticality of choosing a suitable precoding scheme that aligns with user density and network demands to enhance spectral efficiency and augment the overall performance of cell-free massive MIMO systems.

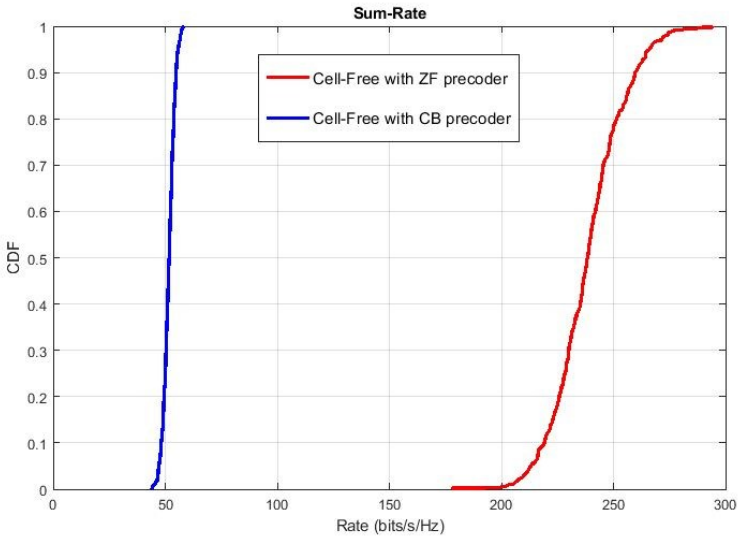

Fig. 4. Shows the CDF of the sum-rate for the suggested method (ZF) precoder compared to the traditional CB precoder with P = 128 and U = 32.

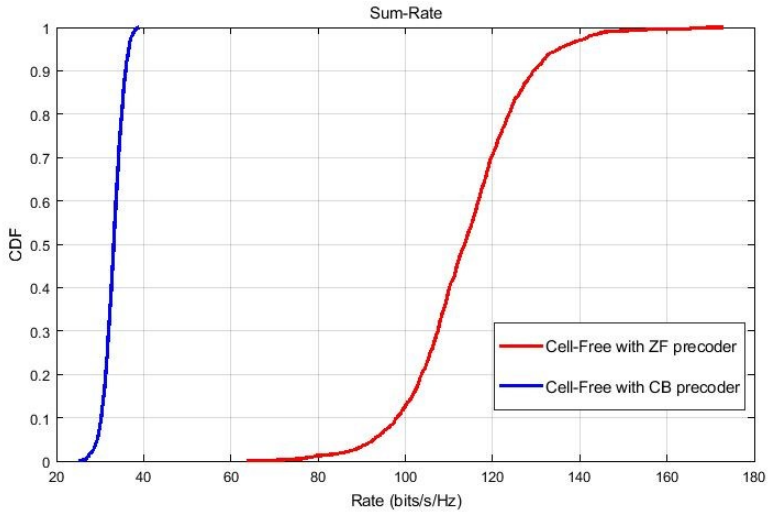

Fig. 5. Shows the CDF of the sum-rate for the suggested method (ZF) precoder compared to the traditional CB precoder with P = 128 and U = 16.

Figures 6 and 7 compare the CDF of the minimum rate for cell-free systems using ZF and CB precoders, highlighting how the number of users affects the minimum achievable rate and demonstrating the superior performance of ZF precoding in maintaining higher minimum rates. Figure 6 indicates that the ZF precoder, markedly excels in minimum rate performance with fewer users compared to the CB precoder. At the median percentile, the ZF precoder secures a rate close to 1 bit/s/Hz, outperforming the CB precoder. The ZF precoder's consistent and effective interference management translates to a superior and dependable minimum rate. In contrast, Figure 7 shows the ZF precoder maintaining enhanced minimum rates at higher percentiles, reflecting its robustness amidst growing user density. Despite some improvement, the CB precoder's performance remains inferior to that of the ZF precoder. Collectively, the data across both figures demonstrate the ZF precoder's consistent ability to achieve higher minimum rates than the CB precoder, irrespective of user density, attributed to its advanced interference management, ensuring reliable minimum rates in cell-free systems.

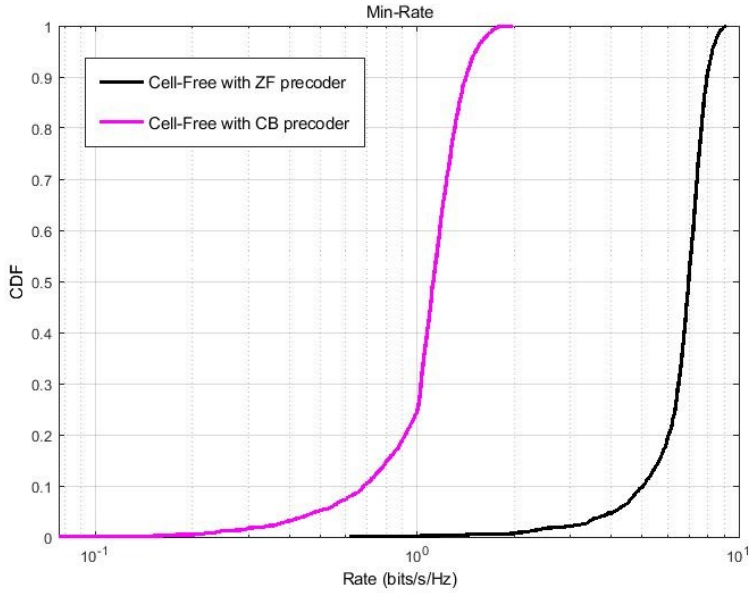

Fig. 6. Shows the CDF of the min-rate for the suggested method (ZF) precoder compared to the traditional CB precoder with P = 128 and U = 16.

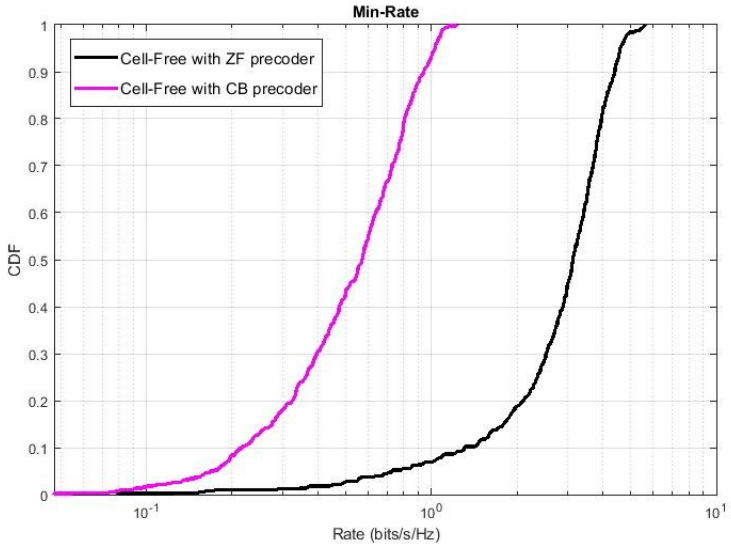

Fig. 7. Shows the CDF of the min-rate for the suggested method (ZF) precoder compared to the traditional CB precoder with P = 128 and U = 32.

7. Conclusion

The downlink performance of cell-free massive MIMO systems was analyzed with respect to the minimum rate for each user and sum-rate. In cell-free massive MIMO systems, all distributed APs simultaneously serve every user, ensuring consistently high-quality service for each user. Employing the max-min criteria, power optimization techniques for cell-free Massive MIMO systems were examined in this work by utilizing ZF and CB precoders. A power allocation strategy was presented for cell-free systems under pilot contamination, which is happening when multiple users share the same pilot signal. The ZF precoding strategy not only demonstrates a substantial performance advantage in terms of sum-rate but also ensures a more consistent and reliable minimum rate for all users across the network. The numerical results presented in this paper indicate a marked performance improvement when using the proposed algorithm for power allocation in cell-free systems with ZF precoding. These findings are consistent with the theoretical predictions, suggesting that the proposed algorithm is both effective and practical for real-world applications. However, the number of users sharing the same pilot is a limitation of the proposed approach.

References

[1] E. Nayebi, A. Ashikhmin, T. L. Marzetta, and H. Yang, "Cell-free massive MIMO systems," in 2015 49th Asilomar Conference on Signals, Systems and Computers, 2015, pp. 695–699. https://ieeexplore.ieee.org/document/7421222

[2] H. Q. Ngo, A. Ashikhmin, H. Yang, E. G. Larsson, and T. L. Marzetta, "Cell-free massive MIMO versus small cells," IEEE Trans. Wirel. Commun., vol. 16, no. 3, pp. 1834–1850, 2017. https://ieeexplore.ieee.org/document/7827017

[3] S. Buzzi and C. D'Andrea, "Cell-free massive MIMO: User-centric approach," IEEE Wireless Communications Letters, vol. 6, no. 6. pp. 706–709, 2017. https://ieeexplore.ieee.org/document/8000355

[4] A. A. I. Ibrahim, A. Ashikhmin, T. L. Marzetta, and D. J. Love, "Cell-free massive MIMO systems utilizing multi-antenna access points," in 2017 51st Asilomar Conference on Signals, Systems, and Computers, 2017, pp. 1517–1521. https://ieeexplore.ieee.org/document/8335610

[5] J. Zhang, Y. Wei, E. Björnson, Y. Han, and X. Li, "Spectral and energy efficiency of cell-free massive MIMO systems with hardware impairments," in 2017 9th International Conference on Wireless Communications and Signal Processing (WCSP), 2017, pp. 1–6. https://ieeexplore.ieee.org/document/8171057

[6] T. C. Mai, H. Q. Ngo, and T. Q. Duong, "Uplink spectral efficiency of cell-free massive MIMO with multi-antenna users," in 2019 3rd International Conference on Recent Advances in Signal Processing, Telecommunications & Computing (SigTelCom), 2019, pp. 126–129. https://ieeexplore.ieee.org/document/8696221

[7] E. Nayebi, A. Ashikhmin, T. L. Marzetta, and B. D. Rao, "Performance of cell-free massive MIMO systems with MMSE and LSFD receivers," in 2016 50th Asilomar Conference on Signals, Systems and Computers, 2016, pp. 203–207. https://ieeexplore.ieee.org/document/7869024

[8] H. Almosa, Y. J. Harbi, M. Al-Dulaimi, and A. Burr, "Performance Analysis of DoA Estimation for FDD Cell Free Systems Based on Compressive Sensing Technique," J. Commun., vol. 18, no. 10, pp. 658–664, 2023. https://www.jocm.us/show-295-1940-1.html

[9] B. D. Van Veen and K. M. Buckley, "Beamforming: A versatile approach to spatial filtering," IEEE assp Mag., vol. 5, no. 2, pp. 4–24, 1988. https://ieeexplore.ieee.org/document/665

[10] E. Björnson, J. Hoydis, and L. Sanguinetti, "Massive MIMO networks: Spectral, energy, and hardware efficiency," Found. Trends® Signal Process., vol. 11, no. 3–4, pp. 154–655, 2017. http://dx.doi.org/10.1561/2000000093

[11] N. Hassan and X. Fernando, "Massive MIMO wireless networks: An overview," Electronics, vol. 6, no. 3, p. 63, 2017. https://www.mdpi.com/2079-9292/6/3/63#

[12] T. L. Marzetta, E. G. Larsson, and H. Yang, Fundamentals of massive MIMO. Cambridge University Press, 2016.

[13] T. L. Marzetta, "Noncooperative cellular wireless with unlimited numbers of base station antennas," IEEE Trans. Wirel. Commun., vol. 9, no. 11, pp. 3590–3600, 2010. https://ieeexplore.ieee.org/document/5595728

[14] O. Elijah, C. Y. Leow, T. A. Rahman, S. Nunoo, and S. Z. Iliya, "A comprehensive survey of pilot contamination in massive MIMO—5G system," IEEE Commun. Surv. Tutorials, vol. 18, no. 2, pp. 905–923, 2015. https://ieeexplore.ieee.org/document/7339665
[15] R. R. Müller, L. Cottatellucci, and M. Vehkaperä, "Blind pilot decontamination," IEEE J. Sel. Top. Signal Process., vol. 8, no. 5, pp. 773–786, 2014. https://ieeexplore.ieee.org/document/6756975
[16] H. Yin, D. Gesbert, M. Filippou, and Y. Liu, "A coordinated approach to channel estimation in large-scale multiple-antenna systems," IEEE J. Sel. areas Commun., vol. 31, no. 2, pp. 264–273, 2013. https://ieeexplore.ieee.org/document/6415397
[17] H. Yin, D. Gesbert, and L. Cottatellucci, "Dealing with interference in distributed large-scale MIMO systems: A statistical approach," IEEE J. Sel. Top. Signal Process., vol. 8, no. 5, pp. 942–953, 2014. https://ieeexplore.ieee.org/document/6812159
[18] H. Yin, L. Cottatellucci, D. Gesbert, R. R. Müller, and G. He, "Robust pilot decontamination based on joint angle and power domain discrimination," IEEE Trans. Signal Process., vol. 64, no. 11, pp. 2990–3003, 2016. https://ieeexplore.ieee.org/document/7420690
[19] M. D. Alrubay and H. Almosa, "Channel Estimation Enhancement in Cell-Free Massive MIMO Systems under Pilot Contamination," vol. 22, pp. 1688–1700, 2024. https://pjlss.edu.pk/articles/2024_1/1688-1700.htm
[20] H. Wang, L. Li, J. Wang, L. Song, Y. Ma, and Z. Zhou, "A transmit precoding scheme for downlink multiuser MIMO systems," in 2011 IEEE Vehicular Technology Conference (VTC Fall), 2011, pp. 1–5. https://ieeexplore.ieee.org/document/6093007
[21] L. Lu, G. Y. Li, A. L. Swindlehurst, A. Ashikhmin, and R. Zhang, "An overview of massive MIMO: Benefits and challenges," IEEE J. Sel. Top. Signal Process., vol. 8, no. 5, pp. 742–758, 2014. https://ieeexplore.ieee.org/document/6798744
[22] T. L. Marzetta, "Noncooperative cellular wireless with unlimited numbers of base station antennas," IEEE Transactions on Wireless Communications, vol. 9, no. 11. pp. 3590–3600, 2010. https://ieeexplore.ieee.org/document/5595728
[23] F. Rusek et al., "Scaling up MIMO: Opportunities and challenges with very large arrays," IEEE Signal Process. Mag., vol. 30, no. 1, pp. 40–60, 2012. https://ieeexplore.ieee.org/document/6375940
[24] E. G. Larsson, O. Edfors, F. Tufvesson, and T. L. Marzetta, "Massive MIMO for next generation wireless systems," IEEE Commun. Mag., vol. 52, no. 2, pp. 186–195, 2014. https://ieeexplore.ieee.org/document/6736761
[25] F. Boccardi, R. W. Heath, A. Lozano, T. L. Marzetta, and P. Popovski, "Five disruptive technology directions for 5G," IEEE Commun. Mag., vol. 52, no. 2, pp. 74–80, 2014. https://ieeexplore.ieee.org/document/6736746
[26] D. Qiao, Y. Wu, and Y. Chen, "Massive MIMO architecture for 5G networks: Co-located, or distributed?," in 2014 11th International Symposium on Wireless Communications Systems (ISWCS), 2014, pp. 192–197. https://ieeexplore.ieee.org/document/6933345
[27] G. N. Kamga, M. Xia, and S. Aïssa, "Spectral-efficiency analysis of massive MIMO systems in centralized and distributed schemes," IEEE Trans. Commun., vol. 64, no. 5, pp. 1930–1941, 2016. https://ieeexplore.ieee.org/document/7386643
[28] U. Madhow, D. R. Brown, S. Dasgupta, and R. Mudumbai, "Distributed massive MIMO: Algorithms, architectures and concept systems," in 2014 information theory and applications workshop (ITA), 2014, pp. 1–7. https://ieeexplore.ieee.org/document/6804225
[29] S. M. Kay, "Statistical signal processing: estimation theory," Prentice Hall, vol. 1, p. Chapter-3, 1993.
[30] E. Nayebi, A. Ashikhmin, T. L. Marzetta, H. Yang, and B. D. Rao, "Precoding and power optimization in cell-free massive MIMO systems," IEEE Trans. Wirel. Commun., vol. 16, no. 7, pp. 4445–4459, 2017. https://ieeexplore.ieee.org/document/7917284
[31] H. Yang and T. L. Marzetta, "Capacity performance of multicell large-scale antenna systems," in 2013 51st Annual Allerton Conference on Communication, Control, and Computing (Allerton), 2013, pp. 668–675. https://ieeexplore.ieee.org/document/6736589
[32] S. Boyd and L. Vandenberghe, Convex optimization. Cambridge university press, 2004.
[33] E. Björnson and L. Sanguinetti, "Scalable cell-free massive MIMO systems," IEEE Trans. Commun., vol. 68, no. 7, pp. 4247–4261, 2020. https://ieeexplore.ieee.org/document/9064545